



ELSEVIER

Contents lists available at ScienceDirect

Comptes Rendus Chimie

www.sciencedirect.com



Full paper / Mémoire

Sensitization of Eu(III) luminescence by donor-phenylethynyl-functionalized DTPA and DO3A macrocycles

Anthony D'Aléo^a, Mustapha Allali^a, Alexandre Picot^a, Patrice L. Baldeck^b,
Loïc Toupet^c, Chantal Andraud^a, Olivier Maury^{a,*}

^a CNRS-École normale supérieure de Lyon, UMR 5182, laboratoire de Chimie, université de Lyon, 46, allée d'Italie, 69007 Lyon, France

^b Laboratoire de spectrométrie physique, université Joseph-Fourier, 38402 Saint-Martin-d'Hères, France

^c Institut de physique-IPR-UMR CNRS 6251, université de Rennes, 1, bâtiment 11A, 35042 Rennes cedex, France

ARTICLE INFO

Article history:

Received 14 December 2009

Accepted after revision 14 January 2010

Available online 1 March 2010

Keywords:

Luminescence

Spectroscopy

Macrocylic ligand

Nonlinear optics

Two-photon absorption

Mots clés :

Luminescence

Spectroscopies

Ligands macrocycliques

Optique non linéaire

Absorption à deux photons

ABSTRACT

The synthesis and complexation to Eu(III) of two macrocyclic ligands functionalized donor-phenylethynyl-moieties as sensitizer is presented. The two ligands based on DTPA bis-amide ($[\text{Eu}(\text{L}^1)]$) and DO3A ($[\text{Na}][\text{Eu}(\text{L}^2)]$) have been chosen because of their increased stability in water for potential applications as luminescent bioprobes for one- or two-photon excited scanning microscopy. The DTPA and DO3A ligands possess oxygen or sulfur donor atoms, respectively, connected to a triethyleneglycol (PEG) chain to ensure the water solubility. The optical properties were studied and reveal that ($[\text{Eu}(\text{L}^1)]$) present a lower brightness than the ($[\text{Na}][\text{Eu}(\text{L}^2)]$) counterpart because of its inner sphere water molecule coordination that quenches the emission. On the other hand, $[\text{Na}][\text{Eu}(\text{L}^2)]$ exhibits excellent spectroscopic properties with high quantum yield $\phi = 0.284$, and brightness $B = 10,220 \text{ M}^{-1} \text{ cm}^{-1}$ (defined as $\varepsilon \cdot \phi$). Unfortunately, the two-photon cross-section of this last complex was measured to be only 4 GM limiting its potential applications to linear microscopy.

© 2010 Académie des sciences. Published by Elsevier Masson SAS. All rights reserved.

R É S U M É

Cet article décrit la synthèse et la complexation à l'euporium (III) de deux ligands macrocycliques de type DTPA bis-amide ($[\text{Eu}(\text{L}^1)]$) et DO3A ($[\text{Na}][\text{Eu}(\text{L}^2)]$) fonctionnalisés par des groupements donneur-phenylène-éthynylène. Ces macrocycles ont été choisis en raison de leur stabilité reconnue dans les milieux biologiques afin de concevoir de nouvelles bio-sondes luminescentes pour la microscopie biphotonique. L'étude des propriétés spectroscopiques de ces deux complexes a mis en évidence l'excellent rendement quantique de luminescence, $\phi = 0,284$ ainsi que la brillance $B = 10\,220 \text{ M}^{-1} \text{ cm}^{-1}$ (définie comme le produit $\varepsilon \cdot \phi$) accrue du composé $[\text{Na}][\text{Eu}(\text{L}^2)]$. Cependant, sa faible section efficace d'absorption à deux photons limitera ses potentialités en microscopie non linéaire.

© 2010 Académie des sciences. Publié par Elsevier Masson SAS. Tous droits réservés.

1. Introduction

Luminescent lanthanide complexes have attracted much recent attention because of their use in a wide variety of bio-imaging applications such as biofluoroimmunoassays [1–3], as biosensors [4–9], or for two-photon

* Corresponding author.

E-mail address: olivier.maury@ens-lyon.fr (O. Maury).

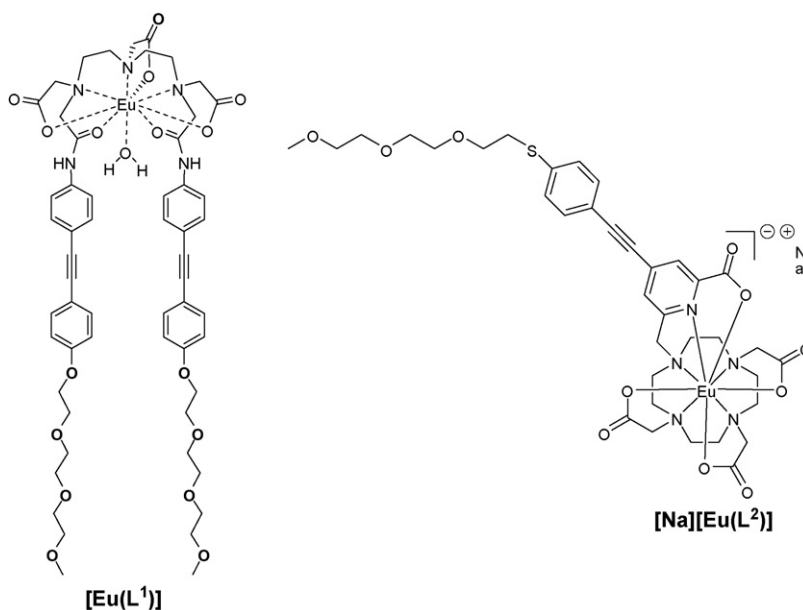
bioprobes for scanning microscopy [10–15]. In most cases, these complexes consist of a lanthanide ion coordinated to a ligand that shields the metal ion from water coordination and bears a sensitizing chromophore which transfers its excitation energy to the luminescent lanthanide ion. The presence of the organic chromophores able to strongly absorb UV-visible light and to transfer this energy to the lanthanide ion overcomes the limitation of an intrinsically small molar absorption coefficient of the forbidden $f-f$ transitions (ϵ about $1\text{--}10\text{ L.Mol}^{-1}.\text{cm}^{-1}$). This so-called “antenna effect” results in the considerable increase of the brightness defined as the product of the luminescence quantum yield and the absorption coefficient, $B = \epsilon.\Phi$. In addition, the luminescence quantum yield and lifetime are highly sensitive to the inner coordination sphere and dramatically decrease when OH vibrators are coordinated. Furthermore, for *in vivo* applications, the ligands have to bind strongly the lanthanide ion in order to form kinetically stable complexes in a biological medium to avoid any release of toxic-free Ln(III) ions.

The unique properties of these ions include line-like emission, long luminescence lifetimes (in the μs –ms range), the sensitivity to the surrounding symmetry and the relative insensitivity of their emission to the presence of dioxygen (that is due to very fast energy transfer from the transferring excited state to the $f-f$ emitting state) [16,17]. Despite extensive research, the optimization of the energy transfer for the sensitization of the lanthanide ion by exciting complexed chromophores is still not fully understood and remains a challenging task. In this respect, the europium ion is an interesting probe since Beeby et al. [18] and Werts et al. [19] have shown that the steady state luminescence spectrum and the luminescence lifetime of the europium ion can be used to evaluate the efficiency of the sensitization process and

therefore understand the limitation residing in the studied systems.

We recently showed that the water soluble functionalized dipicolinate ligand can possess absorption transitions in the UV-visible (up to 400 nm) with high molar absorption coefficient and can efficiently sensitize Eu(III) [12,20], Yb(III) or Nd(III) [20] ions. In the mean time, these complexes present large two-photon cross-section values. This exaltation is induced by intraligand charge transfer (ILCT) state. Unfortunately, despite a stability good enough to make *in vitro* measurements, the previously presented chelators are not stable enough for *in vivo* applications. In the progress of our research, we looked for a new scaffold to improve the stability of the complexes. In this context, we decided to base our complexes on the DTPA [21,22] and DO3A [23,24] macrocyclic units well known to lead to the formation of complexes with enhanced stability in aqueous media.

Here, we report on the synthesis and complexation to Eu(III) of two new ligands featuring donor-phenylethynyl functionalities that are based on DTPA bis-amide ([Eu(L¹)] and DO3A ([Na][Eu(L²)] (Scheme 1). Those ligands possess electron donating oxygen or sulfur donor atoms, respectively, connected to a π -conjugated skeleton to induce a charge transfer transition [20,25] and additional triethyleneglycol (PEG) chain to insure the water solubility. The optical properties were studied and reveal that the DTPA bis-amide derivative ([Eu(L¹)] is much less bright than the DO3A derivative ([Na][Eu(L²)] because of the presence of a coordinated water molecule that quenches the emission. On the other hand, [Na][Eu(L²)] reaches excellent photophysical properties almost as good as our benchmark compound [12]. However, the two-photon cross-section of this complex was measured to be only 4 GM limiting its potentialities for two-photon applications.



Scheme 1. Structures of the investigated europium(III) complexes.

2. Results and discussion

2.1. Synthesis

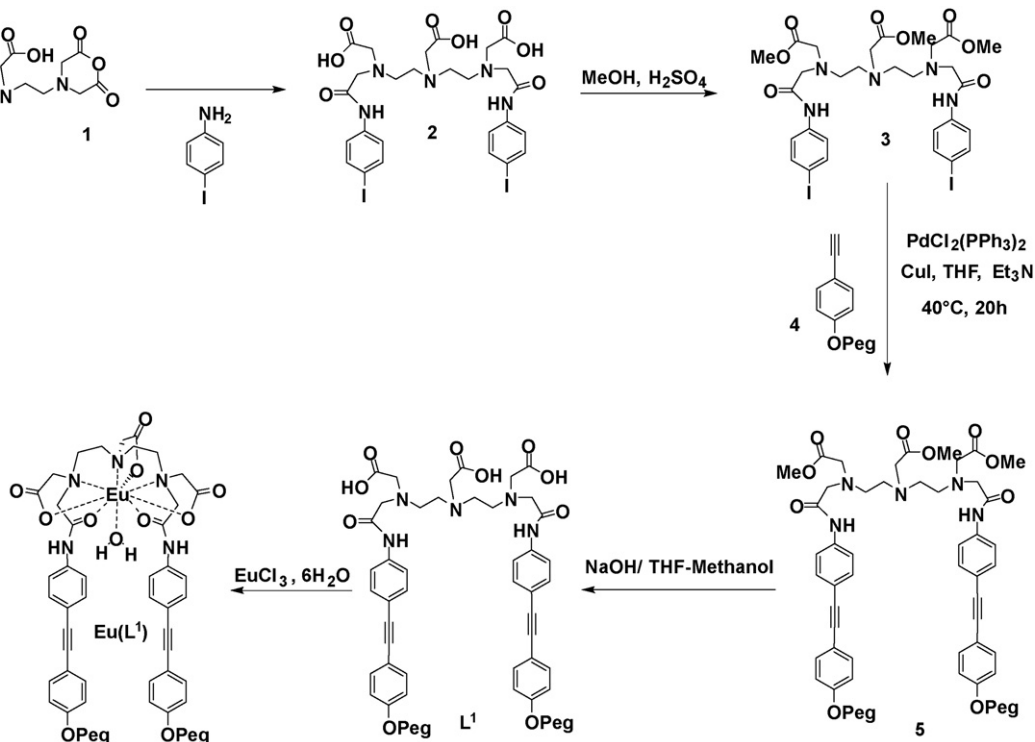
The synthesis of the DTPA derivative (Scheme 2) was readily started with the opening of the bis-anhydride **1** by the addition of 4-iodoaniline giving the DTPA bis-amide derivative **2**. After esterification of the three free carboxylic acid functions, the resulting tri-ester **3** was coupled to the acetylene derivative **4** [26] using a Pd-catalyzed Sonogashira cross-coupling reaction under standard conditions yielding **5** after column chromatography with an acceptable yield (66%). The final ligand **L**¹ was obtained after deprotection of the ester moieties in basic methanol-THF solution (1 M sodium hydroxide). Complete analyzes are compiled in the experimental section. Mixing the ligand **L**¹ with one equivalent of EuCl₃·6H₂O in aqueous solution followed by extraction with dichloromethane leads to the formation of analytically pure [Eu(L¹)]·6H₂O.

The DO3A derivative was prepared starting from the iododipicolinic diester **6** [27] (Scheme 3). The key step of this synthesis was the desymmetrisation of **6** into carboxylic acid-alcohol **7** thanks to a kinetically controlled monoreduction by sodium borohydride at room temperature in methanolic solution. After Sonogashira cross-coupling with **8** [26], the chromophore **9** was obtained in good yield (84%) after column chromatography. The alcohol function was then activated with mesyl chloride (**10**) and further attached to cyclen macrocycle giving the monosubstituted species **11**. The remaining free amine functions of **11** were then alkylated by bromoacetate in basic medium and the final functionalized DO3A derivative

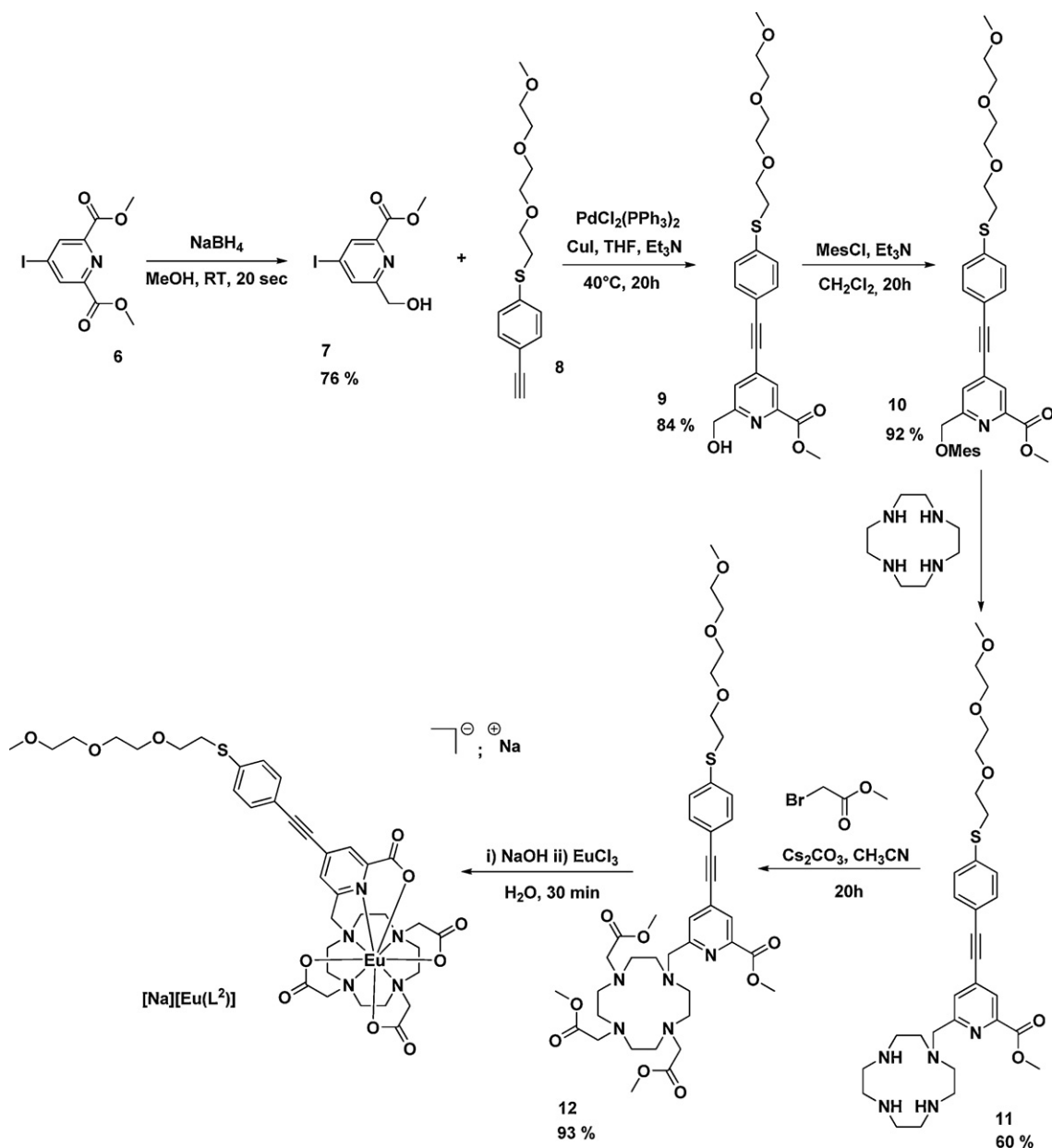
12 was purified using column chromatography on alumina oxide. After saponification of the four ester moieties, a one pot complexation to Eu(III) ion was carried out in a buffered solution at pH = 6.

2.2. Crystal structure of the Eu-DTPA model

Due to the presence of the long PEG chains, we were not able to prepare good quality crystals of [Eu(L¹)]. Therefore, white crystals of the model complex [Eu(**2**)] featuring iodophenyl pendant arm were obtained upon cooling down a hot methanol solution (see experimental section for the complex preparation). The complex crystallized as a methanol adduct with two methanol and one diethyl ether interstitial solvent molecules. At the molecular level (Fig. 1, top), the wrapping of the DTPA ligand around the central Eu(III) ion orientates the two iodophenyl in almost the same direction (the angle (I1N1),(I2N5) is estimated to be 12°). It is worth noting that the two phenyl rings are not parallel and form an angle of 32°, a distortion certainly related to the steric hindrance induced by the coordinated methanol molecule. The central europium ion is non-coordinated by three nitrogen, the carboxylato- and two amido-oxygen atoms, the last position being occupied by an oxygen atom from a methanol molecule. The coordination polyhedron (Fig. 1, bottom) is a distorted tricapped trigonal prism with the Eu, O3, O9, N3 atoms lying in the equatorial plane (maximum standard deviation < 0.1 Å). Such a type of structure is relatively frequent for lanthanide DTPA complexes also dimer formation can be



Scheme 2. Synthetic pathway for the preparation of [Eu(L¹)].



Scheme 3. Synthetic pathway for the preparation of $[\text{Na}][\text{Eu}(\text{L}^2)]$.

observed depending on the sterical hindrance afforded by the DTPA functionalization [28] (Table 1).

2.3. UV-visible absorption spectroscopy

The UV/visible absorption data for each of the Eu(III) complexes in water are depicted in Fig. 2 and all the data are summarized in Table 2. The two complexes possess their lowest absorption transition in the visible with maxima at 300 and 338 nm for $[\text{Eu}(\text{L}^1)]$ and $[\text{Na}][\text{Eu}(\text{L}^2)]$, respectively. This red shift observed for $[\text{Na}][\text{Eu}(\text{L}^2)]$ as compared to $[\text{Eu}(\text{L}^1)]$ will favor the former complex for two-photon applications since measurements are performed using Ti-sapphire laser sources between

700–900 nm (i.e. when doubled: 350–450 nm). Furthermore, the observed cut-off of the UV/visible absorption for $[\text{Eu}(\text{L}^1)]$ (at 350 nm) precludes any measurement of the two-photon excitation spectrum. In addition, the molar absorption coefficients of $[\text{Eu}(\text{L}^1)]$ and $[\text{Na}][\text{Eu}(\text{L}^2)]$ are 17,650 and 36,000 $\text{M}^{-1}\text{cm}^{-1}$, respectively. In this case, the molar absorption coefficient is in favor of $[\text{Na}][\text{Eu}(\text{L}^2)]$ that will give an advantageous brightness for this complex.

2.4. Luminescence of Eu(III) complexes and determination of the sensitization parameters

The steady state emission spectra, the luminescence quantum yields and luminescence lifetimes of the Eu(III)

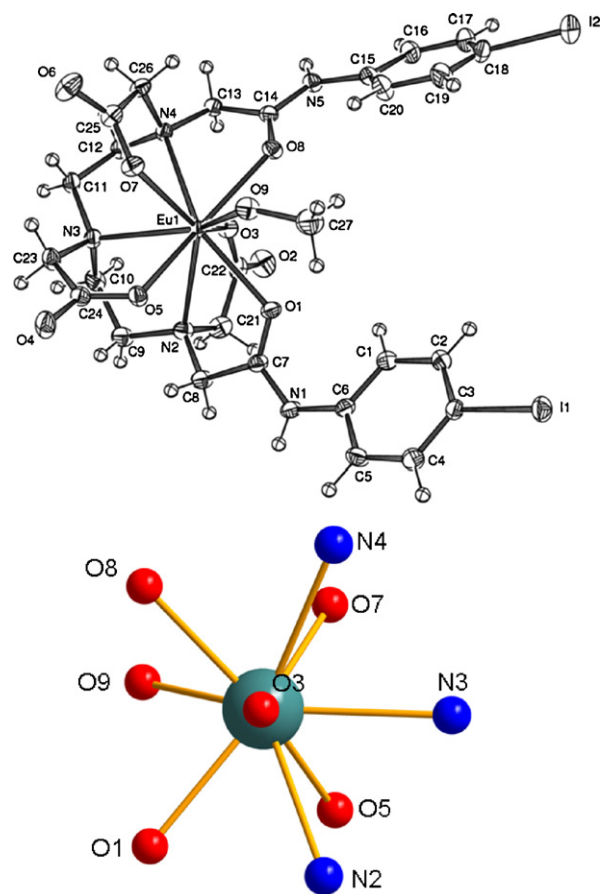


Fig. 1. ORTEP drawing for $[\text{EuL}_2\text{C}_{27}\text{H}_{33}\text{N}_5\text{O}_9 \cdot \text{CH}_3\text{OH}] \cdot 3\text{CH}_3\text{OH} \cdot \text{C}_4\text{H}_{10}\text{O}$. Interstitial solvent molecules were omitted for clarity (top). Coordination polyhedron around the Eu(III) ion (bottom). Selected bond lengths (Å): (amino) Eu-N2 = 2.755(3); Eu-N3 = 2.640(3); Eu-N4 = 2.673(3); (amido) Eu-O1 = 2.485(2); Eu-O8 = 2.481(2); (carboxylato) Eu-O7 = 2.394(2); Eu-O5 = 2.344(2); Eu-O3 = 2.331(3); (methanol) Eu-O9 = 2.483(3).

Table 1

Crystal data and refinement parameters.

Formula	$\text{C}_{34}\text{H}_{55}\text{Eu}_2\text{N}_5\text{O}_{13}$
f.w. ($\text{g}\cdot\text{mol}^{-1}$)	1147.59
Cryst. Syst.	Monoclinic
Space group	P21/n
a (Å)	10.4117(2)
b (Å)	14.7816(4)
c (Å)	26.6463(6)
α ($^\circ$)	90.0
β ($^\circ$)	99.2700(10)
γ ($^\circ$)	90.0
V (Å^3)	4047.35(16)
Z	4
T (K)	120
λ (MoK α) (Å)	0.71069
D ($\text{g}\cdot\text{cm}^{-3}$)	1.883
μ (mm^{-1})	3.143
R(F) ^a , I > 1 σ (Fo)	0.037
R _w (F ²) ^b , I > 1 σ (Fo)	0.094
S	0.67
Rint	0.056
θ max	32.25
h	-15 → 14
k	-22 → 13
l	-37 → 38
Parameters	496
Measured reflections	37666
Independent reflections	12950
Reflections with I > 2.0 σ (I)	9882
$\Delta\rho_{\text{min}}$	-2.095 e Å ⁻¹
$\Delta\rho_{\text{max}}$	2.217 e Å ⁻¹

$$^a R(F) = \frac{\sum ||F_o| - |F_c||}{\sum |F_o|}$$

$$^b R_w(F) = \frac{\sum [w((F_o^2 - F_c^2)^2)]}{\sum wF_o^4}^{1/2}$$

complexes were measured in water (Table 2). The relevant radiative and non-radiative parameters were also determined following the works of Werts et al. [19] and Beeby et al. [18], and a complete summary of these data are reported in Table 3. As can be seen from Fig. 3, the spectra of the two Eu(III) complexes are very similar with intense $J = 2$ and $J = 4$ transitions. In both spectra, all transitions are split in numerous transitions revealing the low symmetry

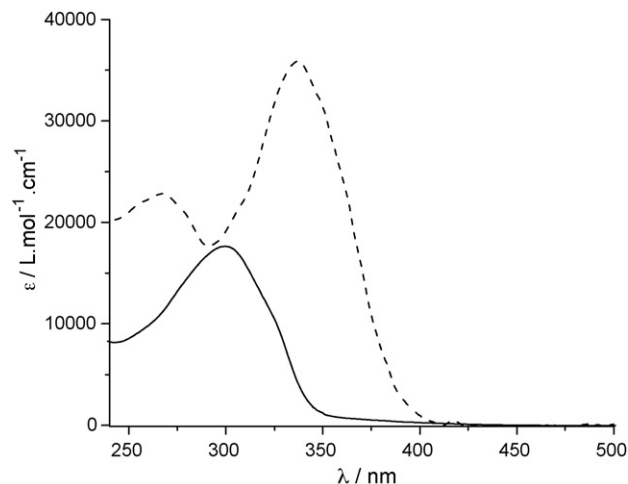


Fig. 2. UV/visible absorption spectra in water of $[\text{Eu}(\text{L}^1)]$ (—) and $[\text{Na}][\text{Eu}(\text{L}^2)]$ (---).

Table 2
Optical data in water for the two complexes.

Complex	Absorption			Luminescence			$B \text{ M}^{-1}\text{cm}^{-1}$
	λ^{max} nm	$\epsilon \text{ M}^{-1}\text{cm}^{-1}$	Cut-off nm	ϕ_{Eu}	$\tau_{\text{Eu}}^{\text{Ha}}$ ms	$\tau_{\text{Eu}}^{\text{Da}}$ ms	
[Eu(L¹)]	300	17,650	350	0.019	0.59	1.87	335
[Na][Eu(L²)]	338	36,000	405	0.284	1.39	n.d.	10,220

^a $\tau_{\text{Eu}}^{\text{H}}$ and $\tau_{\text{Eu}}^{\text{D}}$ represent the luminescence lifetime in H₂O and D₂O, respectively.

Table 3
Calculated luminescence parameters τ_{R} , k_{r} , Σk_{nr} , η_{Eu} , and η_{sens} for the two investigated Eu(III) complexes using the experimental quantities ϕ_{Eu} , τ_{Eu} and $[I(0,1)/I_{\text{tot}}]$ in water.

Complex	ϕ_{Eu}	$\tau_{\text{Eu}}/\text{ms}$	$\tau_{\text{R}}/\text{ms}$	η_{Eu}	η_{sens}	$[I(0,1)/I_{\text{tot}}]$	$k_{\text{r}}/\text{s}^{-1}$	$\Sigma k_{\text{nr}}/\text{s}^{-1}$
[Eu(L¹)] ^a	0.019	0.59	4.58	0.129	0.147	0.148	218	1477
[Na][Eu(L²)]	0.284	1.39	4.24	0.328	0.866	0.137	236	483
[Eu(L¹)] ^{a,b}	0.078	0.98	3.86	0.254	0.305	0.152	259	761

^a Not taking the $J = 3$ into account because of the overlap with the 2λ of the excitation.

^b Measured in dichloromethane solution.

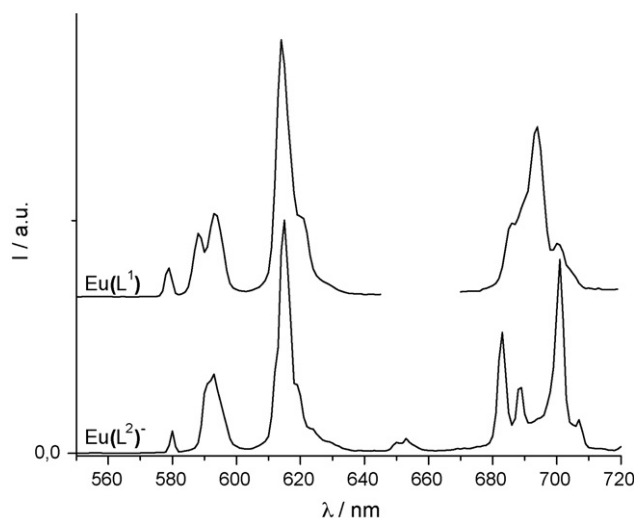


Fig. 3. Normalized luminescence spectra (on $J = 2$) of **[Na][Eu(L²)]** (bottom, $\lambda^{\text{ex}} = 335 \text{ nm}$) and **[Eu(L¹)]** (top, $\lambda^{\text{ex}} = 325 \text{ nm}$) in water.

of those complexes [29]. In the two cases, the $J = 0$ seems to be a single transition which is typical of the presence of only one species in solution (full-width-at-half-maximum of the $J = 0$ transitions are 750 and 450 cm^{-1} for **[Eu(L¹)]** and **[Na][Eu(L²)]**, respectively). This observation is confirmed by the presence of a mono-exponential decay for both samples. The luminescence quantum yields measured in water are very different about 2% for **[Eu(L¹)]** up to 28% for **[Na][Eu(L²)]** with luminescence lifetimes of 0.59 and 1.39 ms, respectively. Such differences in terms of luminescence quantum yields and lifetimes suggest the presence of water molecules in the inner sphere of **[Eu(L¹)]** while the complex **[Na][Eu(L²)]** most likely presents a saturated coordination sphere. In order to determine the number of water molecules in the inner sphere of **[Eu(L¹)]**, the luminescence lifetime was also measured in deuterated water, yielding a value of 1.87 ms, which is far higher than that in water. The q number can therefore be obtained (Table 3) using the improved phenomenological Horrocks

equation [30], revealing a $q = 1.2$ (substantially one water molecule) in agreement with the crystal structure of the model complex **[Eu(2)]** containing one solvent molecule. Similar water molecule coordination has already been observed in related complexes [31].

To understand the limitation and advantage of such ligands, the radiative and non-radiative parameters were determined. As can be seen in Table 3, the symmetry of both complexes are almost equivalent giving identical ratio of intensities between the $J = 1$ and the whole spectrum. Consequently, both complexes exhibit identical radiative lifetimes (τ_{r}) and radiative decay rate (k_{r}) [31]. Here, it has to be highlighted that both complexes possess a coordination number of 9 giving the possibility of a similar symmetry around the metal (in the case of **[Eu(L¹)]**, the ninth site being occupied by the water molecule). Therefore, for **[Eu(L¹)]**, the large decrease of the luminescence lifetime induces a drop of the europium centered efficiency ($\eta_{\text{Eu}} = 0.129$) compared to

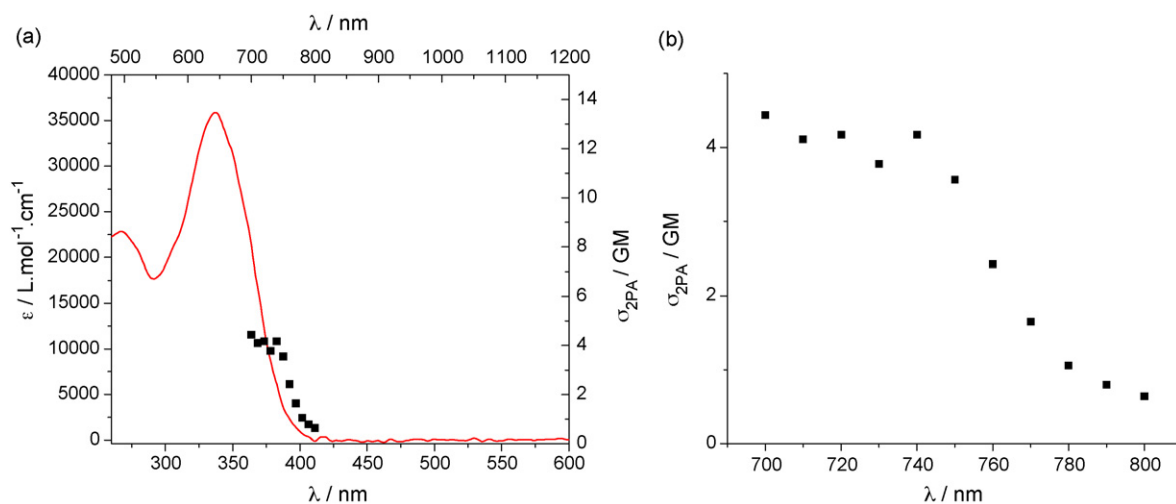


Fig. 4. a: two-photon excitation spectrum of $[\text{Na}][\text{Eu}(\text{L}^2)]$ in water solution (\blacksquare , upper abscissa). Superimposed on this plot is the single-photon absorption spectrum in wavelength doubled scale ($-$, lower abscissa); b: two-photon excitation spectrum of $[\text{Na}][\text{Eu}(\text{L}^2)]$ in water solution (\blacksquare).

$[\text{Na}][\text{Eu}(\text{L}^2)]$ ($\eta_{\text{Eu}} = 0.328$) that is followed by a large difference in the non-radiative decay rate (483 s^{-1} vs. 1477 s^{-1} for $[\text{Na}][\text{Eu}(\text{L}^2)]$ and $[\text{Eu}(\text{L}^1)]$, respectively). As can be seen in the Table 3, all parameters related to the europium centre (τ_{Eu} and η_{Eu}) are very low in the case of $[\text{Eu}(\text{L}^1)]$. This can be explained by the inner sphere water molecule bound to the metal cation (also increasing the non-radiative decay rate ($\sum k_{\text{nr}}$)). It is worth noting that the sensitization efficiency (η_{sens}), that is independent of the presence of inner sphere water molecule, is low for $[\text{Eu}(\text{L}^1)]$ (0.147) while it is almost quantitative for $[\text{Na}][\text{Eu}(\text{L}^2)]$ (0.866). In the dichloromethane solution, this sensitization efficiency remains rather low ($\eta_{\text{sens}} = 0.305$) proving the inefficiency of L^1 ligand to induce Eu(III) luminescence.

2.5. Two-photon absorption properties

Since $[\text{Eu}(\text{L}^1)]$ has its UV/visible absorption cut-off at 350 nm and is poorly emissive ($\phi = 0.019$), no measurement of the two-photon excitation spectrum was performed. On the other hand, the two-photon absorption cross-sections ($\sigma_{2\text{PA}}$) of $[\text{Na}][\text{Eu}(\text{L}^2)]$ have been determined in water using the two-photon excited fluorescence technique in the 700–900 nm wavelength range with a femtosecond Ti-Sapphire pulsed laser source, according to the experimental protocol described by Xu and Webb (coumarin-307 as a standard) [32]. The two-photon excitation spectrum matches the wavelength-doubled scale single-photon one (Fig. 4a). This similarity indicates that the low lying excited state in energy is one- and two-photon allowed and confirms that the europium luminescence is induced by a two-photon antenna effect with a similar photophysical sensitization process (the same excited states are involved in the one- or two-photon sensitization process). As can be seen in Fig. 4, the $\sigma_{2\text{PA}}$ found for $[\text{Na}][\text{Eu}(\text{L}^2)]$ in water is rather small compared to the value reported for the europium (III) dipicolinate derivatives [12,33] revealing a maximum of 4 GM. This can

be partially rationalized by the presence of only one chromophore while three of such chromophores were present in the previously cited studies.

3. Conclusion

In conclusion, this article reported the first attempts at the design of europium complexes featuring high stability in biological media and excellent one- or two-photon brightness, which are the key requirements for a luminescent bioprobe for biphotonic microscopy. To that end, well-known macrocycles, namely DTPA and DO3A, were functionalized by already described two-photon antenna chromophores. In the case of DTPA-bis amide derivative $[\text{Eu}(\text{L}^1)]$, the presence of one water molecule in the first coordination sphere results in a strong quenching of the europium luminescence. On the other hand, the functionalized DO3A complex $\text{Na}[\text{Eu}(\text{L}^2)]$ presents an excellent one-photon brightness, but the presence of only one antenna chromophore reduces dramatically its two-photon absorption efficiency. New macrocycles functionalized by several two-photon antenna chromophores are currently being prepared in our group towards the design of this new generation of Ln-based bioprobes.

4. Experimental

4.1. Crystal structure analysis

The samples were studied on a Oxford Diffraction Xcalibur Saphir 3 diffractometer with graphite monochromatized $\text{MoK}\alpha$ radiation. Cell parameters were obtained with Denzo and Scalepack with 10 frames (ψ rotation: 1° per frame). The structure was solved with SIR-97 [34], which reveals the non hydrogen atoms of structure. After anisotropic refinement, many hydrogen atoms may be found with a Fourier Difference. The whole structure was refined with SHELXL97 [35] by the full-matrix

least-square techniques (use of F magnitude; x, y, z, α_{ij} for C, N and O atoms, x, y, z in riding mode for H atoms). ORTEP views were made with PLATON 98 [36]. All calculations were performed on a Silicon Graphics Indy computer. Crystallographic datum for the structural analysis has been deposited with the Cambridge Crystallographic Data Centre, CCDC 601476.

4.2. UV/visible absorption measurements

UV/visible absorption measurements were recorded on a JASCO V550 absorption spectrometer. The spectra were corrected using a solution of water as a reference.

4.3. Luminescence measurements

The luminescence spectra were measured using a Horiba-Jobin Yvon Fluorolog-3 spectrofluorimeter (see the preceding article for details). Phosphorescence lifetimes ($> 30 \mu\text{s}$) were obtained by pulsed excitation using an FL-1040 UP xenon lamp. Luminescence decay curves were fitted by least-squares analysis using Origin. Fluorescence quantum yields, Q , were measured in a diluted solution with an optical density lower than 0.1 using the following equation: $Q_x/Q_r = [A_r(\lambda)/A_x(\lambda)][n_x^2/n_r^2][D_x/D_r]$, where A is the absorbance at the excitation wavelength (λ), n is the refractive index, and D is the integrated luminescence intensity. The “r” and “x” stand for reference and sample. Here, references are $\text{Ru}(\text{bpy})_3 2\text{Cl}$ complexes in a water solution ($Q_r = 0.028$) [37] and $[\text{Na}]_3[\text{EuL}^{1\text{C}}_3]$ ($Q_r = 0.157$) [12] for each complex.

4.4. Two-photon excited luminescence measurements

The TPA cross-section spectra were obtained by up-conversion fluorescence using a Ti:sapphire femtosecond laser in the range of 700–900 nm. The excitation beam (5 mm diameter) is focalized with a lens (focal length 10 cm) at the middle of the fluorescence cell (10 mm). The fluorescence, collected at 90° to the excitation beam, was focused into an optical fiber (diameter 600 μm) connected to an Ocean Optics S2000 spectrometer. The incident beam intensity was adjusted to 50 mW in order to ensure an intensity-squared dependence of the fluorescence over the whole spectral range. The detector integration time was fixed to 1 s. Calibration of the spectra was performed by comparison with the published 700–900 nm Coumarin-307 two-photon absorption spectrum60 (Coumarin-307 quantum yield 0.56 in ethanol). The measurements were done at room temperature in dichloromethane and at a concentration of 10^{-4} M.

4.5. General procedure

4 and **8** were prepared following the published procedure [33]; all other starting materials were commercially available. All solvents for synthesis were analytic grade. For the spectroscopy, spectroscopic grade solvents were used. NMR spectra (^1H and ^{13}C) were recorded at room temperature on a BRUKER AC 200 operating at 200.13 and 50.32 MHz for ^1H and ^{13}C , respectively. Data

are listed in parts per million (ppm) and are reported relative to tetramethylsilane (^1H and ^{13}C); residual solvent peaks of the deuterated solvents were used as an internal standard. Low resolution mass spectrometry was carried out on an Agilent 1100 Series LC/MSD apparatus. High-resolution mass spectrometry measurements and elemental analyses were performed at the Service Central d'Analyse du CNRS (Vernaison, France).

4.6. Synthesis

1. In a 250 mL round bottom flask, a suspension of DTPA (49 g, 125 mmol) in acetic anhydride (53 mL, 560 mmol) and dry pyridine (62 mL, 770 mmol) was heated at 65°C , while stirring for 24 h. After cooling to room temperature, the precipitate formed was filtered off and then washed with diethyl ether. After drying under vacuum, pure DTPA-bis(anhydride) **4** was obtained (43 g, 120 mmol, 96%). ^{13}C -NMR ($[d_6]$ -DMSO): 50.78, 51.72, 52.71, 54.73, 165.88, 171.82 ppm.

2. In a 50-ml round bottom flask, iodoaniline was solubilized in DMF (20 mL). Pyridine was added to the solution followed by **1**. The solution was stirred for 1–2 h at room temperature. The DMF was removed by adding toluene, and the solid obtained was cleaned twice with dichloromethane (2×150 mL). Yield 85%. ^1H -NMR (200.13 MHz, $[d_6]$ -DMSO): 10.12 (d, 2H), 7.55 (d, $^3J = 8.8$ Hz, 4 H), 7.45 (d, $^3J = 8.8$ Hz, 4H), 3.43 (m, 10H), 2.95 (m, 4H), 2.90 (m, 4H).

3. In a 250-ml round bottom flask, **2** was suspended in anhydrous MeOH (150 mL), 2 mL of concentrated H_2SO_4 was added and the solution was refluxed for 16 h. After a cooling period, the acid was neutralised by adding NaHCO_3 . The solution was filtered and the solvent was evaporated. Yield 95%. ^1H -NMR (200.13 MHz, CDCl_3): 9.77 (bs, 2H, NH), 7.57 (d, $^3J = 6.8$ Hz, 4H), 7.40 (d, $^3J = 6.8$ Hz, 4H), 3.68 (m, 9H), 3.48 (m, 10H), 2.71 (m, 8H); ^{13}C -NMR (50.332 MHz, CDCl_3): 177.06, 175.80, 174.23, 172.30, 141.64, 141.44, 126.05, 125.95, 90.86, 50.78, 50.36, 51.63, 51.21, 52.91, 52.49, 52.06, 55.00; m/z 838 (MH^+ requires 838), 860 (MNa^+ requires 860).

5. In a 100-mL schlenk flask, **3** (0.25 g, 0.30 mmol) was dissolved in a mixture of THF and triethylamine (15 mL/15 mL). The solution was thoroughly degassed by argon bubbling for 20 min and **4** [33] (0.75 mmol, 2.5 equiv.), copper iodide (0.2 equiv.) and $(\text{Ph}_3\text{P})\text{PdCl}_2$ (0.1 equiv.) were added under a flux of argon. The reaction was stirred at 40°C for 14 h. The compound was purified by column chromatography on silica using gradient ethyl acetate/methanol (9/1 to 7/3) as eluent. This yields a brown oil (0.22 g, 66%). ^1H -NMR (200.13 MHz, CDCl_3): $\delta = 9.82$ (bs, 2H), 7.59 (d, $^3J = 8.6$ Hz, 4H), 7.44 (m, 8H), 6.88 (d, $^3J = 8.7$ Hz, 4H), 4.12 (t, $^3J = 5.6$ Hz, 4H), 3.84 (t, $^3J = 5.5$ Hz, 4H), 3.75 (s, 9H), 3.40–3.72 (m, 26H), 3.54 (m, 2H), 3.36 (s, 6H), 2.74 (m, 8H); EI-MS: $[\text{M} + \text{H}]^+$: 1110, $[\text{M} + \text{Na}]^+$: 1132.

L. In a 100-mL round bottom flask, **5** (0.236 g, 0.230 mmol) was dissolved in 30 mL of methanol and stirred at room temperature. Subsequently, 10 mL of a 1 M aqueous sodium hydroxide solution is added and the reaction is stirred at room temperature for 2 h. The solution is extended to 50 mL by adding water and the

solvents, the crude material is purified by chromatography on aluminum oxide (CH₂Cl₂: MeOH 39/1) to afford the product as a bright yellow oil (1.08 g, 93%). ¹H NMR (500 MHz, CDCl₃): 7.92 (s, 1H), 7.44 (s, 1H), 7.33 (d, ³J = 8.4 Hz, 2H), 7.19 (d, ³J = 8.4 Hz, 2H), 3.87 (s, 3H), 3.67 (s, 3H), 3.59 (t, ³J = 6.8 Hz, 2H), 3.52–3.46 (m, 12H), 3.44–3.36 (m, 2H), 3.24 (s, 3H), 3.06 (t, J = 6.8 Hz, 2 H), 3.2–2.2 (m, 24H); ¹³C-NMR (50.332 MHz, CDCl₃): 173.5, 172.4, 165.0, 159.2, 147.7, 139.5, 134.0, 132.2, 129.0, 127.5, 125.3, 118.0, 96.2, 85.9, 71.7, 70.31, 70.29, 70.26, 69.4, 59.1, 58.8, 55.2, 54.9, 53.0, 52.2, 51.9, 50.2, 32.0; λ_{max} (H₂O)/nm 333 (ε/dm³ mol⁻¹ cm⁻¹ 27400); LRMS m/z: 816 (MH⁺ requires 816), 838 (MNa⁺ requires 838); HRMS m/z: 816.3848 (MH⁺ calcd for C₄₀H₅₈N₅O₁₁S requires 816.3854).

[Na][Eu(L²)]. To a stirred solution of **12** (122 mg, 0.15 mmol, 1 eq) in H₂O (10 mL) in a 50-mL round bottom flask, is added NaOH (36 mg, 0.9 mmol, 6 eq). After stirring for 1 h at 50 °C, the solution is cooled down to room temperature and acidified to pH = 6 by addition of 0.1 M HCl solution. At that stage, a solution of EuCl₃·6H₂O (66 mg, 0.18 mmol, 1.2 eq) in H₂O (10 mL) is slowly added while the pH of the reaction is kept at pH = 6 by addition of 0.1 M NaOH solution. Once the pH of the reaction is stable, the reaction is stirred for an additional 20 h at 75 °C. λ_{max} (H₂O)/nm 334 (ε/dm³ mol⁻¹ cm⁻¹ 36100); LRMS m/z: 910 (MHH⁺ requires 910), 932 (MHNa⁺ requires 932), 948 (MHK⁺ requires 948), 954 (MNaNa⁺ requires 954); HRMS m/z: 954.1859 (MNaNa⁺ calcd for C₃₆H₄₅EuN₅Na₂O₁₁S requires 954.1844).

Acknowledgments

The authors thank the ANR LnOnL NT05-3_42676 for financial support and for grants to AD and MA. We are also grateful to ENS Lyon for AP's grant.

References

- [1] H.L. Handl, R.J. Gillies, *Life Sci* 77 (2005) 361.
- [2] S. Petoud, S.M. Cohen, J.C.G. Bünzli, K.N. Raymond, *J. Am. Chem. Soc* 125 (2003) 13324.
- [3] E.G. Moore, A.P.S. Samuel, K.N. Raymond, *Acc. Chem. Res* 42 (2009) 542.

- [4] B. Song, G. Wang, M. Tan, J. Yuan, *J. Am. Chem. Soc* 128 (2006) 13442.
- [5] S.M. Borisov, O.S. Wolbeis, *Anal. Chem* 78 (2006) 5094.
- [6] M.I. Stich, S. Nagl, O.S. Wolbeis, U. Henne, M. Schaeferling, *Adv. Funct. Mater* 18 (2008) 1399.
- [7] D. Parker, *Coord. Chem. Rev* 205 (2000) 109.
- [8] M.S. Tremblay, M. Halim, D. Sames, *J. Am. Chem. Soc* 129 (2007) 7570.
- [9] S. Pandya, J. Yu, D. Parker, *Dalton Trans* (2006) 2757.
- [10] C. Andraud, O. Maury, *Eur. J. Inorg. Chem* (2009) 4357.
- [11] A. D'Aléo, G. Pompidor, B. Elena, J. Vicat, P.L. Baldeck, L. Toupet, R. Kahn, C. Andraud, O. Maury, *Chem. Phys. Chem* 8 (2007) 2125.
- [12] A. Picot, A. D'Aléo, P.L. Baldeck, A. Grishine, A. Duperray, C. Andraud, O. Maury, *J. Am. Chem. Soc* 130 (2008) 1532.
- [13] G.L. Law, K.L. Wong, C.W.Y. Man, W.T. Wong, S.W. Tsao, M.H.W. Lam, K.S. Lam, *J. Am. Chem. Soc* 130 (2008) 3714.
- [14] F. Kielar, A. Congreve, G.L. Law, E.J. New, D. Parker, L.L. Wong, P. Castreno, J. De Mendoza, *Chem. Commun* (2008) 2435.
- [15] F. Kielar, G.L. Law, E.J. New, D. Parker, *Org. Biomol. Chem* 6 (2008) 2256.
- [16] J.C.G. Bünzli, C. Piguat, *Chem. Soc. Rev* 34 (2005) 1048.
- [17] J.C.G. Bünzli, *Acc. Chem. Res* 39 (2006) 53.
- [18] A. Beeby, L.M. Bushby, D. Maffeo, J.A.G. Williams, *J. Chem. Soc. Dalton Trans* (2002) 48.
- [19] M.H.V. Werts, R.T.F. Jukes, J.W. Verhoeven, *Phys. Chem. Chem. Phys* 4 (2002) 1542.
- [20] A. D'Aléo, A. Picot, A. Beeby, J.A.G. Williams, B. Le Guennic, C. Andraud, O. Maury, *Inorg. Chem* 47 (2008) 10258.
- [21] G.R. Choppin, D.R. Peterman, *Coord. Chem. Rev* 174 (1998) 283.
- [22] Z. Jaszberenyi, E. Toth, T. Kalai, R. Kiraly, L. Burai, E. Brucher, A.E. Merbach, K. Hideg, *Dalton Trans* 4 (2005) 694.
- [23] K. Kumar, C.A. Chang, M.F. Tweedle, *Inorg. Chem* 32 (1993) 587.
- [24] R.A. Poole, G. Bobba, M.J. Cann, J.C. Frias, D. Parker, R.D. Peacock, *Org. Biomol. Chem* 3 (2005) 1013.
- [25] A. Picot, F. Malvolti, B. Le Guennic, P.L. Baldeck, J.A.G. Williams, C. Andraud, O. Maury, *Inorg. Chem* 46 (2007) 2659.
- [26] W. Denk, J.H. Strickler, W.W. Webb, *Science* 248 (1990) 73.
- [27] A. Picot, C. Feuvrie, C. Barsu, F. Malvolti, B. Le Guennic, H. Le Bozec, C. Andraud, O. Maury, *Tetrahedron* 64 (2008) 399.
- [28] Y. Inomata, T. Sunakawa, F.S. Howell, *J. Mol. Struct* 648 (2003) 81.
- [29] A. D'Aléo, J. Xu, K. Do, G. Muller, K.N. Raymond, *Helv. Chim. Acta* 92 (2009) 2439.
- [30] R.M. Supkowski, W.D. Horrocks, *Inorg. Chim. Acta* 340 (2002) 44.
- [31] C.G. Gulgas, T.M. Reinenke, *Inorg. Chem* 44 (2005) 9829.
- [32] C. Xu, W.W. Webb, *J. Opt. Soc. Am. B* 13 (1996) 481.
- [33] A. D'Aléo, A. Picot, P.L. Baldeck, C. Andraud, O. Maury, *Inorg. Chem* 47 (2008) 10269.
- [34] A. Altomare, M.C. Burla, M. Camalli, G. Carcano, C. Giacovazzo, A. Guagliardi, A.G.G. Moliterni, G. Polidori, R.J. Spagna, *Appl. Crystallogr* 31 (1998) 74.
- [35] G.M. Sheldrick, in: *SHELX 93, Program for the refinement of crystal structures*, University of Göttingen, Germany, 1993.
- [36] A.L. Spek, in: *PLATON, A multipurpose crystallographic tool*, University, Utrecht, The Netherlands, 1998.
- [37] K. Nakamaru, *Bull. Chem. Soc. Jpn* 55 (1982) 2697–2705.